An MR-compatible force sensor based on FBG technology for biomedical application.

P. Saccomandi-*IEEE, Student Member*, M.A. Caponero, A. Polimadei, M. Francomano, D. Formica-*IEEE Member,* D. Accoto-*IEEE Member*, E. Tamilia-*IEEE, Student Member*, F. Taffoni-*IEEE Member,* G. Di Pino and E. Schena-*IEEE Member*

***Abstract*—Fiber Bragg Grating (FBG) technology is very attractive to develop sensors for the measurement of thermal and mechanical parameters in biological applications, particularly in presence of electromagnetic interferences. This work presents the design, working principle and experimental characterization of a force sensor based on two FBGs, with the feature of being compatible with Magnetic Resonance. Two prototypes based on different designs are considered and characterized: 1) the fiber with the FBGs is encapsulated in a polydimethylsiloxane (PDMS) sheet; 2) the fiber with the FBGs is free without the employment of any polymeric layer. Results show that the prototype which adopts the polymeric sheet has a wider range of measurement (4200 mN vs 250 mN) and good linearity; although it has lower sensitivity (≈0.1 nm·N^{-1} vs 7 nm·N^{-1}). The sensor without polymeric layer is also characterized by employing a differential configuration which allows neglecting the influence of temperature. This solution improves the linearity of the sensor, on the other hand the sensitivity decreases.**

The resulting good metrological properties of the prototypes here tested make them attractive for the intended application and in general for force measurement during biomedical applications in presence of electromagnetic interferences.

I. Introduction

Historically optical fibers were firstly employed in medicine to illuminate internal organs during endoscopic procedures. During the years the same technology has been adopted to perform other tasks, such as laser treatments, and to develop transducers for monitoring parameters of interest for both therapeutic and diagnostic purposes [1]. The optical fiber technology has been largely employed in medicine to monitor mechanical and thermal parameters [2-7], and it is also attractive for force sensors development. This is due to the good metrological properties of fiber optic sensors (FOSs), such as, sensitivity, accuracy and low zero drift, among others. Beyond the already well-established applications in industrial and medicine, the immunity from electromagnetic interferences makes FOSs attractive for several applications that take place inside, or close to, the magnetic resonance scanner during Magnetic Resonance Imaging (MRI) procedures [8]. The growing interest in the development of MRI-compatible sensors is motivated by the constant increase of exams based on MRI and the introduction of new procedures performed under MRI-guidance in clinical practice. In this scenario FOSs can be useful to improve both surgical procedures outcome and to allow patient monitoring (e.g., measure of the temperature in subjects undergoing MRI-guided thermal procedures [9], to the assessment of deflection and force on needles during MRI-guided procedures, and to the estimation of physiological parameters [10]. Moreover, both intensity – based [11] and Fiber Bragg Grating (FBG)-based [12] FOSs have been recently applied in the field of tactile sensing.

This paper presents the design of an FBG-based, MRI-compatible force sensor and its static characterization. The sensor is developed employing two configurations in order to have different measurement ranges and sensitivities. Moreover, the performances of a further configuration based on a differential approach have been experimentally assessed.

This work can be considered the first step toward realizing an FBG-based, MRI-compatible sensor for monitoring forces applied during object manipulation. The MRI compatibility allows performing experiments during functional MRI (fMRI) studies to investigate the relationship between the intensity of applied force and the general pattern of human brain activity and the reactions to force stimuli of patients undergoing fMRI procedures. Future innovation of the sensors here proposed can allow developing tactile sensors.

II. Sensor design and theory of operation

FBGs are periodic changes of the refractive index of a fiber optic; they are etched within the fiber core by exposure to an intense optical interference pattern [13]. When interrogated with a polychromatic radiation, the FBG reflects only a narrow range of wavelengths. The central wavelength of the range is called the Bragg wavelength, λ_B, and depends on the spatial period of grating, Λ, and on the effective refraction index of the core, η_{eff}:

$$\lambda_B = 2 \cdot \Lambda \cdot \eta_{eff} \tag{1}$$

FBGs are employed as sensors for temperature and strain. In fact, the shift of λ_B, i.e., $\Delta\lambda_B$, depends on the change in both Λ and η_{eff}, which can be caused by fiber strain, ε, and temperature variation, ΔT, as expressed in (2):

P. Saccomandi and E. Schena are with the Unit of Measurements and Biomedical Instrumentation, Center for Integrated Research, Università Campus Bio-Medico di Roma, Via Álvaro del Portillo, 21-00128- Rome-Italy, [p.saccomandi][e.schena][s.silvestri]@unicampus.it.

A. Polimadei and M. A. Caponero are with Photonics Micro- and Nano-structures Laboratory, Research Centre of Frascati, ENEA, Via E. Fermi, 45 –00044–Frascati -Italy, [michele.caponero][andrea.polimadei] @enea.it.

M. Francomano, D. Formica, D. Accoto, E. Tamilia, F. Taffoni and G. Di Pino are with the Unit of Biomedical Robotics and Biomicrosystems, Center for Integrated Research, Università Campus Bio-Medico di Roma, Via Álvaro del Portillo, 21-00128- Rome-Italy, [m.francomano][d.formica][d.accoto][e.tamilia][f.taffoni][g.dipino]@unicampus.it.

978-1-4244-7929-0/14/$26.00 ©2014 IEEE

$$\frac{\Delta\lambda_B}{\lambda_B} = c_\varepsilon \cdot \varepsilon + c_T \cdot \Delta T \qquad (2)$$

Where c_ε and c_T are the strain and the temperature coefficient, respectively.

Since λ_B is related to the period of Bragg grating (Λ), the basic design of an FBG-based force sensor requires the force causing a strain in the fiber Bragg grating. Two main factors must be taken into account during the design: 1) the loss of the reflected light due to the fiber microbending, which can cause error in Bragg wavelength measurement; and 2) the chirping phenomenon, which is due to a non-uniform strain distribution along the whole grating length, leading to a distortion of λ_B.

Some configurations are employed to design FBG-based force sensors, either minimizing or avoiding those effects mentioned above. Heo and Coauthors, for instance, presented a design which avoided microbending and any strain dishomogeneity along the grating [12].

The proposed sensor is based on a sensing element consisting of a fiber optic with two FBGs reflecting two separate Bragg peaks (i.e., about 1545 nm and 1548 nm at environmental temperature). The fiber acts as a cantilever fixed at the two extremities to a plastic box, *ad hoc* designed using SolidWorks Software and manufactured by means of a 3D printer (Fig. 1). The distance between the two extremities has been fixed to 1.1 cm and the two 0.1 cm-long FBGs are placed at a distance of 0.5 cm each other. The plastic box design allows preventing excessive deflection of the fiber avoiding fiber rupture and unwarranted light loss: its maximum value is limited by the short distance between the fiber center and the plastic (i.e., 0.45 cm). The employment of two FBGs, placed at short distance from each other, is motivated by the influence of temperature on their response, as shown in (2). Therefore, the use of two FBGs can allow to reject the influence of temperature on sensor response. This finding can be obtained by developing differential configuration which uses the Bragg wavelength shift of both the FBGs.

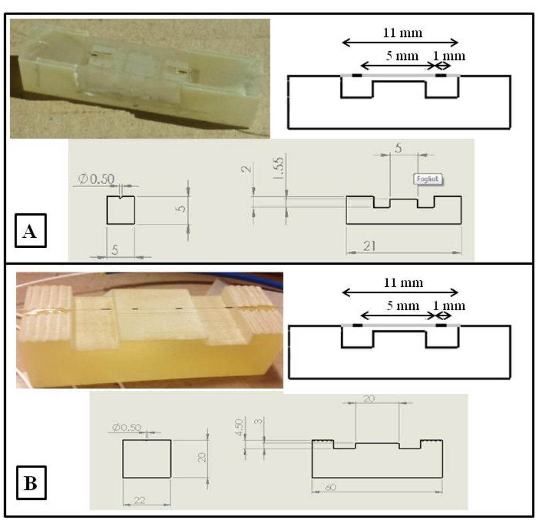

Figure 1. Prototype, CAD and schematic of A) the force sensor with fiber encapsulated in PDMS; B) the force sensor without PDMS encapsulation.

Two different prototypes of the sensor have been developed:

A) in the first prototype (Fig. 1.A), the optical fiber, fixed to the plastic box with the geometry schematically reported in Fig. 1.A, has been encapsulated in a layer of polydimethylsiloxane (PDMS), obtained by mixing the pre-polymer components in a 10:1 (base: curing agent) ratio. The PDMS has been poured into a 3D printed plastic box, housing the optical fiber, and it has been cured at room temperature for 24 hours. In this way, the applied force acts on the PDMS layer, which shields the fiber with a thickness of 1 mm.

B) in the second prototype (Fig. 1.B), the fiber is fixed to the plastic box as in the first configuration, but without the employment of any PDMS. In this case, a force acting perpendicularly to the fiber, deflects the fiber which can be schematically described as a 11 mm length cantilever. The fiber deflection causes a strain of the two FBGs, leading to a $\Delta\lambda_B$: the higher the force, the higher the deflection, hence the higher the λ_B increase.

III. Experimental Set-up

The static calibration of the two prototypes has been carried out in order to analyze their metrological properties (e.g., range of measurement, sensitivity, discrimination threshold and range of linearity). The experimental set up is shown in Fig. 2 and employs a mechanical testing system (series 5900, Instron, Fig. 2.A) which allows applying controlled compression load to the sensor. The testing system is equipped with a load cell (range of measurement up to 5 N, accuracy=±0.5% of reading, Fig. 2.B) which measures and records with a sample frequency of 50 Hz the applied force; the system also measures the strain of the specimen under test. Two screw grips were used to hold the sensor under test (Fig. 2.C). The fiber optic with the two inscribed FBGs (Fig. 2.D) allows the communication between the sensing element and the Optical Spectrum Analyzer (Optical Sensing Interrogator, sm125, Micron Optics). The spectrum was collected by a PC using a LabVIEW-based software.

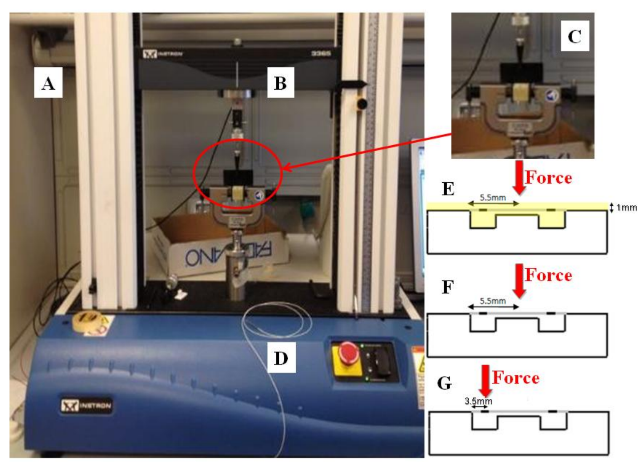

Figure 2. A) Mechanical testing system; B) load cell; C) sensor and system to fix the sensor when compression loads are applied; D) fiber optic; E-G) points of force application.

Employing the set up described in Fig. 2, three different experiments have been performed: 1) force applied between the two FBGs encapsulated in the layer of PDMS (Fig. 2.E); 2) force applied between the two FBGs without PDMS (Fig. 2.F); 3) force applied on one FBGs in the prototype without PDMS (Fig. 2.G).

IV. Results

Figure 3 shows the relationship between the $\Delta\lambda_B$ of the two FBGs and the force applied to the center of the fiber in the case of encapsulated FBGs (Fig. 2.E) and without PDMS (Fig. 2.F).

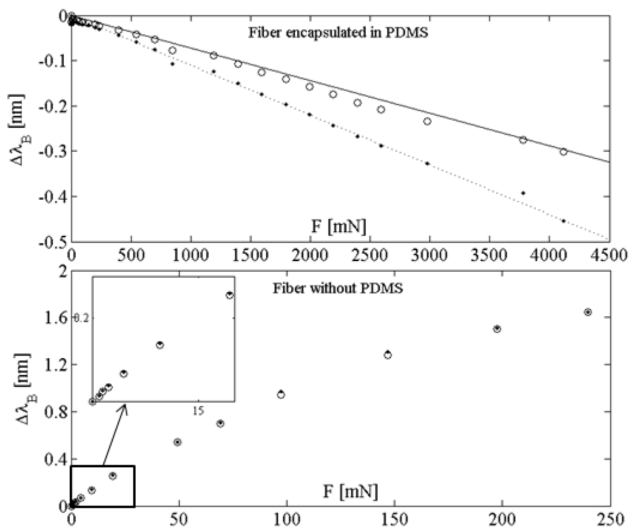

Fig. 3. Experimental characterization of the force sensor. A) sensor with the fiber encapsulated within a PDMS layer: relationship between FBGs output and the applied force. The best fitting lines are also shown; B) Relationship between the FBGs output and the applied force in the sensor without PDMS. The zoom of the linear range (up to 25 mN) is shown in the upper left corner.

The sensor encapsulated in the PDMS layer (Fig. 3.A) shows a linear response in the whole range of measurement (up to 4200 mN). The good linearity is confirmed by the high value of correlation coefficient (R^2>0.97) for both the FBG outputs. Moreover, the linear decrease of FBG outputs with F shows a slight asymmetry, probably due to PDMS inhomogeneity (the slopes of the two best fitting lines are -0.072 nm·N^{-1} and -0.110 nm·N^{-1}, respectively). The slope can be considered the sensitivity of the force sensor.

The sensor without PDMS shows a non-linear response in the range of measurement up to 250 mN (Fig. 3.B) and a narrow range of linearity (see zoom in Fig. 3.B) up to 25 mN; the main advantage respect to the configuration with PDMS is the higher sensitivity (+6.8 nm·N^{-1}). Figure 3.A shows that, when FBGs are encapsulated in PDMS, the axial force applied as in Fig. 2.E results in a PDMS compression in proximity to the plastic box wall. As a consequence the grating period is compressed by the PDMS, hence λ_B decreases with the force intensity. Differently, in the prototype without PDMS (Fig. 2.F), the axial force causes a traction of the FBGs and, therefore, the increase of $\Delta\lambda_B$ (Fig. 3.B).

Further experiments have been carried out on the configuration without PDMS by applying the force to the center of one FBG (Fig. 2.G). As expected, the response of the two FBGs is not symmetric: the FBG placed below the applied force undergoes higher strain, hence higher $\Delta\lambda_B$, than the second one. The experimental results show that the difference between the two $\Delta\lambda_B$ ($\Delta\lambda_{B1\text{-}2}$) is linearly related to the applied force (Fig. 4) in the whole range of calibration (up to 250 mN), as confirmed by the high correlation coefficient (R^2≈0.98).

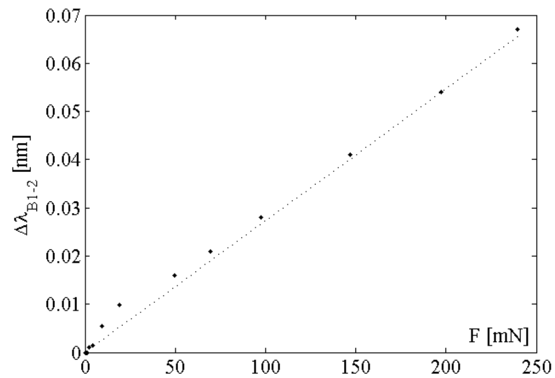

Fig. 4. Response of force sensor without PDMS. The output of the measurement system is considered the difference between the $\Delta\lambda_B$ of the two FBGs, and the application point of the force is below to one of the two FBGs.

As observable, the main drawback of this solution is the decrease of sensitivity (+0.273 nm·N^{-1}) with consequent worsening of the discrimination threshold of the sensor: in this configuration the sensor is not able to discriminate force lower than about 5 mN, with respect to a threshold of about 2 mN obtained by employing a single FBG output and applying the force to the center of the fiber (Fig. 3.B). Despite the weakening of some performances, this differential configuration can be employed to compensate effects induced on the FBGs by external environment (e.g., temperature changes), and also to linearize the sensor response.

The main static characteristics of the sensor considering the three configurations are shown in Table I.

TABLE I. Characteristics of the three configurations. The sensitivity (S) is considered as the mean sensitivity in the whole range of measurement

Metrological characteristics	**Configuration**		
	With PDMS (Fig. 2.E)	Without PDMS (Fig. 2.F)	Differential configuration (Fig. 2.G)
S [nm·N^{-1}]	-0.072÷-0.110	6.8	0.27
Discrimination threshold [mN]	≈80	<2	≈5
Range of measurement [mN]	≈4200	≈250	≈250
Range of linearity [mN]	≈4200	≈25	≈250

V. Discussion and Conclusion

This study presents the design and characterization of an FBG-based force sensor. The sensor was prototyped in two configurations. The configuration with the fiber encapsulated in a PDMS layer shows good linearity, and a wider range of measurement (up to 4200 mN) than the configuration without PDMS (range of measurement up to 250 mN). On the other hand this second configuration presents a high sensitivity which allows discriminating low force (<10 mN). A change in the position of applied force (i.e., below an FBG instead of the center of the fiber, see Fig. 2.E and F) and considering a differential output allows improving the linearity of the sensor's response in the configuration with PDMS; on the other hand this solution causes a decrease of sensitivity.

The light loss and the chirping phenomenon can be considered negligible in the range of force employed during calibration. The good properties of the sensor, the chance to adjust the range of measurement and sensitivity by changing sensor geometry and the characteristics of the polymeric sheet, and its MRI-compatibility motivates the interest in this sensing principle to develop tactile sensor. Moreover, the flexibility of fiber optic and their low size should allow to develop flexible senor [14,15]. Future innovations of these sensors have to comply with integration of FBG in the elastic glove which cover hand prosthesis, being fiber optic based sensors particularly prone to be insensitive to any magneto-electrical noise produced by the motors embedded in the mechatronic device.

REFERENCES

[1] S. Silvestri and E. Schena, "Optical-fiber measurement systems for medical applications," in Optoelectronics Devices and Applications, edited by P. Predeep (InTech, 2011), 205–224.

[2] E. Schena, P. Saccomandi and S. Silvestri, "A high sensitivity fiber optic macro-bend based gas flow rate transducer for low flow rates: Theory, working principle, and static calibration," *Rev. Sci. Instrum*., vol. 84, 2013.

[3] P. Saccomandi, E. Schena, F. Giurazza, R. Del Vescovo, M. A. Caponero, L. Mortato et al., "Temperature monitoring and lesion volume estimation during double-applicator laser-induced thermotherapy in ex vivo swine pancreas: A preliminary study," *Lasers Med Sci*, vol. 29, no. 2, pp. 607-14, 2014.

[4] F. Taffoni, D. Formica, P. Saccomandi, G. Di Pino and E. Schena, "Optical Fiber-Based MR-Compatible Sensors for Medical Applications: An Overview," *Sensors*, vol. 13, pp. 14105-14120, 2013.

[5] E. Schena, P. Saccomandi, and S. Silvestri, "A high sensitivity fiber optic macro-bend based gas flow rate transducer for low flow rates: Theory, working principle, and static calibration," *Rev Sci Instrum*, vol. 84, no. 2, pp. 024301, 2013.

[6] P. Saccomandi et al., "Theoretical assessment of principal factors influencing laser interstitial thermotherapy outcomes on pancreas," *Proc. 34rd Annu. International Conf. IEEE Eng Med Biol Soc*, San Diego, 2012, pp. 5687-5690.

[7] E. Schena, P. Saccomandi, M. Mastrapasqua and S. Silvestri "An optical fiber based flow transducer for infant ventilation: Measurement principle and calibration," *MeMeA 2011-IEEE International Symposium on Medical Measurements and Applications, Proceedings,* Bari, Italy, pp. 5966648.

[8] P. Polygerinos, D. Zbyszewski, T. Schaeffter, R. Razavi, L. D. Seneviratne, K. Althoefer, "MRI-compatible fiber-optic force sensors for catheterization procedures," *IEEE Sensors J*, vol. 10, no. 10, 1598-608, 2010.

[9] E. Schena, P. Saccomandi, F. Giurazza, M. A. Caponero, L. Mortato, F. M. Di Matteo, F. Panzera, R. Del Vescovo, B. Beomonte Zobel, and S. Silvestri, "Experimental assessment of CT-based thermometry during laser ablation of porcine pancreas," *Phys Med Biol*, vol.. 58, pp. 5705-16, 2013.

[10] L. Dziuda, F. W. Skibniewski, M. Krej, and P. M. Baran, "Fiber Bragg grating-based sensor for monitoring respiration and heart activity during magnetic resonance imaging examinations", *J Biomed Opt*, vol. 18, pp. 0570061-14, 2013.

[11] P. Nath, S. Neog, R. Biswas, and A. Choudhury, A. "All Fiber-Optic Sensor for Monitoring Pressure Fluctuations in ON/OFF State," IEEE *Sensors J*, vol. 13, no. 4, pp. 1148-52, 2013

[12] J. S. Heo, J.A. Chung, and J. J. Lee, "Tactile sensor arrays using fiber Bragg grating sensors," *Sensor Actuator*, vol. 126, pp. 312-27, 2013.

[13] K. O. Hill and G. Meltz G, "Fiber Bragg Grating Technology Fundamentals and Overview," *J. Lightwave Technol.*, vol. 15, pp. 1263-76, 1997

[14] D. Accoto, E. Schena, M. Cidda, M. T. Francomano, P. Saccomandi, and S. Silvestri, "A micro opto-mechanical displacement sensor based on micro-diffraction gratings: Design and characterization," *Conf Proc IEEE Eng Med Biol Soc*, pp. 4714-7, 2013.

[15] M. Moscato, E. Schena, P. Saccomandi, M. T. Francomano,D. Accoto, E. Guglielmelli and S. Silvestri, "A micromachined intensity-modulated fiber optic sensor for strain measurements: Working principle and static calibration," *Conf Proc IEEE Eng Med Biol Soc*, pp. 5790-3, 2012.